

PETGraphDB: A Property Evolution Temporal Graph Data Management System

Jinghe Song, Zongyu Zuo, Xuelian Lin, Yang Wang, and Shuai Ma*

School of Computer Science and Engineering, Beihang University

XueYuan Road #37, Beijing, China, 100191

{songjh, zuozy, linxl, yangwangcs, mashuai}@buaa.edu.cn

Abstract—Temporal graphs are graphs whose nodes and edges, together with their associated properties, continuously change over time. With the development of Internet of Things (IoT) systems, a subclass of the temporal graph, i.e., Property Evolution Temporal Graph, in which the value of properties on nodes or edges changes frequently while the graph’s topology barely changes, is growing rapidly. However, existing temporal graph management solutions are not oriented to the Property Evolution Temporal Graph data, which leads to highly complex data modeling and low-performance query processing of temporal graph queries. To solve these problems, we developed PETGraphDB, a data management system for Property Evolution Temporal Graph data. PETGraphDB adopts a valid-time temporal property graph data model to facilitate data modeling, supporting ACID features with transactions. To improve temporal graph query performance, we designed a space-efficient temporal property storage and a fine-granularity multi-level locking mechanism. Experimental results show that PETGraphDB requires, on average, only 33% of the storage space needed by the current best data management solution. Additionally, it achieves an average of 58.8 times higher transaction throughput in HTAP workloads compared to the best current solutions and outperforms them by an average of 267 times in query latency.

Index Terms—temporal graph, temporal property graph, data management, transaction processing

I. INTRODUCTION

Graphs are data structures frequently used to model and analyze complex real-world systems [1], [2]. When real-world systems change over time, dynamic graphs are generated, known as temporal graphs [3], whose nodes, edges, and properties on nodes or edges change over time and reflect alterations in the structure and function of real-world systems [4], [5]. The ability of a temporal graph to incorporate temporal information makes it valuable for numerous applications and research areas, such as infectious disease spread [6], information dissemination [7], hot route discovery [8], and graph pattern mining [5], [9]. Temporal graphs ensure a degree of flexibility that would be unattainable in static graphs, enhancing our ability to control them [10].

With the rapid proliferation of IoT sensors, IoT systems are generating large volumes of a special type of temporal graphs, referred to as Property Evolution Temporal Graph (briefly as PETG), that has a relatively stable topology but rapidly changing property values on nodes and edges. Fig. 1 illustrates an example temporal graph of a traffic system. Roads in the city are represented as directed edges (arrow lines) of the graph and intersections as nodes (black circles). The road can be

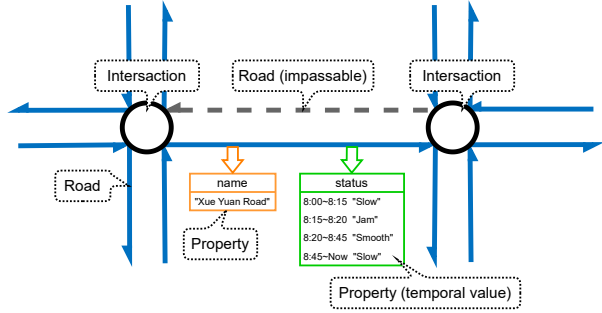


Fig. 1. Example of traffic network model by temporal property graph, including 2 intersections connecting 14 roads

passable (blue solid line) or impassable (gray dashed line). The attributes of a road are considered as properties (boxes) of the corresponding edge. Some attributes do not change with time (yellow box), such as the name and length of the road, while others may update according to time (green box), such as the jam status of roads. In this example, the structure of the road network of a city may occasionally change when a road becomes impassable (or recovers) due to traffic control and other reasons on a daily basis, while the travel time of roads is influenced by the roads’ vehicle flow and changes on a minute-by-minute basis.

PETG data provides new insights into the analysis of the functional dynamics of IoT systems. However, managing PETG data remains challenging due to its distinct data features and access features (see Table I). From a data perspective, (1) most updates are changes in property value rather than topological. In the Energy [11] and Traffic [9] datasets, the portion of property value updates can be as large as 99.9% of total updates, while the others are few; (2) the amount of data in the same time span is much larger (Traffic [9] dataset has an average of 19.5M updates in a day, while the Twitter [13] data only has 767K updates); and (3) there is a large portion of redundant data in the property updates. In the Traffic [9] dataset, the “jam status” of some roads may remain “smooth” during the night. The redundancy ratio of some properties can be as high as 0.8 in some PETG datasets. From the data access perspective, PETG data management should be able to (1) handle large volume data updating and supporting valid-time rather than transaction-time, (2) execute queries that dig into a range of history on a specific entity (referred to as Entity-

TABLE I
DATA (ACCESS) FEATURES OF SOME TEMPORAL GRAPH DATASETS (- FOR NO REPORTED)

Features\Dataset	PETG		Wiki [12]	Other temporal graph data in related work				
	Energy [11]	Traffic [9]		Stack [12]	CitiBike [12]	Twitter [13]	Weibo [13]	Web [13]
Time span (days)	1096	214	2320	2774	90	90	1095	365
graph size (# nodes/edges)	1.5K/2.2K	80K/110K	-	-	-	7.5M/-	27.7M/-	133.6M/-
# events (topology change)	3.7K	190K	8.9M	66.0M	2.5M	69.1M	4.927B	5.641B
# events (property change)	39M	1.39B	0	0	0	0	0	0
# events per day	320K	19.5M	3.8K	23.8K	27K	767K	178K	42K
portion (property to total)	$\geq 99.9\%$	$\geq 99.986\%$			0%			
property redundancy ratio	0.05-0.5	0.2-0.8			-			

History query) rather than the snapshot query, and (3) keep the correctness and efficiency of concurrent read and write.

Motivations: Currently, the solutions for managing temporal graph data include the use of temporal relational databases [14], graph databases [15]–[17], temporal graph databases [18], [19], and temporal graph analysis systems [12], [13], [20]–[25]. However, the lack of consideration of the features and access patterns of PETG data leads to several limitations in current solutions.

Limitation 1: In-intuitive modeling. Current solutions force users to implement application-level logic that transforms PETG data into the native model of their underlying systems and rewrites temporal graph queries into the operations the systems actually support. In addition, the valid time of data in databases can not be updated by users, increasing the flexibility of managing temporal graph data.

Limitation 2: Large space usage. IoT sensors may upload PETG data with redundancy during a relatively long period. However, current solutions do not provide a semantically safe way to eliminate these redundancies, resulting in a significant waste of disk space.

Limitation 3: High query latency. Querying PETG data stored in current systems requires extra processes, which “filter” the graph topology from a mixed storage of graph topology updates and property change updates in (temporal) graph databases, or “construct” the graph topology through multi-table join in (temporal) relational databases. These can lead to high latency when performing temporal graph queries that frequent access topology data.

Limitation 4: Poor transaction performance. Currently, (1) existing temporal graph analysis systems lack transaction support and cannot be used for applications requiring complete transaction management (ACID properties); and (2) locking mechanisms in existing (temporal) relational/graph database systems do not consider the features of PETG data and its queries, resulting in overly coarse-grained locks, which cause frequent mutual waiting and deadlock issues, leading to high transaction latency and low transaction success ratio.

Contributions: In response to the above problems, this paper presents PETGraphDB, a temporal graph data management system oriented to Property Evolution Temporal Graphs (PETG). The main contributions of this paper are as follows:

(1) We design a temporal property graph data model and a query language, providing an intuitive, flexible, and effective

way to model and operate PETG data. This model defines constraints in PETG data to efficiently and safely eliminate redundant information. In addition, this model is fully backward compatible with the widely used property graph data model [26], making it easier for users familiar with graph databases to manage PETG data.

(2) We develop a temporal graph data management system PETGraphDB. The system natively supports PETG data and ACID properties, equips a space-efficient temporal property storage engine that is primarily designed for Entity-History queries, and provides a fine-granularity multi-level locking mechanism to maximize its transaction throughput.

(3) We test the performance of PETGraphDB and the existing temporal graph data management solutions on three datasets. The experimental results show that the storage space occupied by PETGraphDB is an average of 67% less than the best existing solution, and its transaction throughput on HTAP workloads is 58 times higher than that of the best existing solution, while the query latency of PETGraphDB surpasses existing solutions by 267 times on average.

II. RELATED WORK

Based on the underlying techniques, we identify four types of solutions that are commonly used to manage temporal graph data: temporal relational database-based solutions [14], graph database-based solutions [15]–[17], [27], temporal graph databases [18], [19] and temporal graph analysis systems [12], [13], [20]–[25].

1) *Temporal relational database:* The SQL:2011 standard [28] includes temporal features by supporting tense-related functions and a new class of tables called temporal tables, with two extra timestamp columns representing the row’s time start and end. Although the standard defines three types of temporal tables, only transaction-time temporal table is widely supported because it is easy to implement. Nepal [14] is a fault location system for VNF/SDN networks, using virtual machines in the data center as network nodes and network connections between virtual machines as edges. It uses PostgreSQL and its Temporal Tables extension for data storage. Nodes and edges are separately stored in temporal tables and are dynamically joined in the query of graph topology. For path queries, Nepal compiles them into batch SQL join queries. Solutions based on temporal relational databases suffer from performance degradation in topological queries

due to their multi-table joins when reconstructing the graph topology. Moreover, current solutions only support transaction time rather than valid-time, making these solutions unsuitable in scenarios where the data validity time is inconsistent with the time when the data is written to the database.

2) *Graph database*: The graph database is currently a technical solution mainly used to store and manage topology evolution temporal graph data. Cattuto [15] studied the method of using the Neo4j database to store and query social network information over time. It explicitly modeled time as a node and added a model transformation layer to transform temporal graph queries into graph queries. Debrouvier [16] models temporal properties on vertices as additional vertices attached to them, and splits edges with temporal properties to multiple edges. Campos [17] stores time as a property value in the graph database, and the properties are upgraded to “property vertices”. It also provides a SQL-like query language and a method of compiling it into a Cypher query. These solutions require extra access to multiple vertices when updating a temporal property value, which is less efficient. For queries that contain time predicates, index acceleration must be used to achieve acceptable performance. Wu [27] provides a two-stage method to convert a temporal graph into a static graph for the temporal shortest path query. The converted graph loses some information from the original temporal graph, such as the invariance of vertices, and does not consider the property change of nodes in the temporal graph. Graph database solutions introduce extra vertices and edges, which not only increase storage consumption but also hinder the performance of time-related operations.

3) *Temporal graph database*: Aion [18] and AeonG [19] enhance the query of temporal graphs with native graph databases by recording the history of graph updates. Aion [18] highlights a critical challenge that the optimal storage strategy is highly workload- and graph-specific, leading to approaches whose performance is optimal only in parts of the query space. Aion employs two different storage structures, one for the Snapshot query and the other for the Entity-History query, resulting in redundant storage of the same data. It also introduces inefficiencies due to the overhead in the data writing process. AeonG [19] uses hybrid storage structures to manage the “current state” of the graph and the history of the graph separately, which introduces performance degradation for supporting temporal features. These temporal graph databases [18], [19] primarily support transaction-time but lack support for valid-time, which is essential for representing the real-world validity of data. Additionally, these systems are primarily designed for temporal graphs characterized by topology evolution. Moreover, solutions based on existing temporal relational, graph and temporal graph database systems are limited by the underlying system, which does not provide time-related locking mechanisms, resulting in overly coarse-grained locks and low concurrency efficiency.

4) *Temporal graph analysis system*: Wang [29] divided the temporal graph analysis system into two types of systems based on optimization goals: snapshot query and topology

traversal query. Most of the earlier research was oriented to snapshot queries and aimed at rapid analysis of large-scale temporal graphs, including Kineograph [25], Chronons [24], and ImmortalGraph [13]. These systems consider the data locality of time and graph structure in memory and disk storage, and design iterative calculation batch scheduling algorithms based on this locality. DeltaGraph [22] designs an index structure to support snapshot queries of large-scale temporal graph data. G* [23] designed a distributed index and a shared computing acceleration mechanism to support complex queries for distributed analysis and calculation of large-scale temporal graphs. ChrononGraph [21] is optimized for topology traversal queries and aims to analyze the information difference of temporal graph data at different time points. Later, new temporal graph analytical systems GRADOOP [20] and Clock-G [12] support both types of queries at the same time. These systems are all oriented towards data analysis of temporal graphs with topological evolution in which nodes or edges are continuously added or deleted, while the property values of nodes/edges almost remain unchanged, and they do not provide transaction support and fault recovery capabilities necessary for data management.

5) *Summary*: Managing property evolution temporal graph data would involve problems of complex modeling using graph and (temporal) relational databases, poor transaction support using temporal graph analysis systems, and a lack of valid-time support using temporal graph databases. Moreover, issues like large disk space consumption and low query performance may arise because the data features and access features of PETG data are not considered in these systems. These problems raise the threshold for users to manage temporal graph data.

III. DATA MODEL AND QUERY LANGUAGE

This section presents the temporal property graph model and the operators and query language based on this model. We also present a set of commonly used PETG queries that can be implemented by the operators.

A. Temporal Property Graph Data Model

The property graph model [26] provides a flexible and intuitive way to represent complex relationships and attributes in graph data, where both nodes and edges may have associated key-value pairs as properties. The value of properties can be of multiple types, allowing for rich and detailed descriptions.

The temporal property graph model extends the property graph model [26] by adding a new type of property whose value represents a temporal changed value sequence. For simplicity, we call properties whose values are not affected by time *non-temporal property* and properties with temporal values *temporal property*, respectively.

The timeline of a temporal property is represented by a sequence of non-decomposable, consecutive time units termed *chronons* [30]. *Chronons* and its related concept *time interval* [31], are derived from the domain of temporal relation database and are briefly described below.

Definition 1 (Chronon [30]): A chronon τ is a nondecomposable, discrete unit of time of some fixed, minimal duration [30]. *Chronons* are of identical duration, which is defined by users when creating the temporal property. For example, a *chronon* can be a second, an hour, a month, or a year. Note that a special chronon *NOW* is later than any other chronon.

Definition 2 (Time Interval [31]): A time interval $\bar{\tau} = [\tau_s, \tau_e]$ on a timeline is formed by a series of continuous chronons [31], representing the duration of time starting from chronons τ_s (inclusive) to τ_e (exclusive), satisfying $\tau_s < \tau_e$.

Definition 3 (Time Interval Series): A *Time Interval Series* Ψ is an ordered set composed of $(\bar{\tau}, \text{value})$ tuples:

$$\Psi = \langle (\bar{\tau}_1, \text{value}_1), (\bar{\tau}_2, \text{value}_2), \dots, (\bar{\tau}_n, \text{value}_n) \rangle$$

The tuple $(\bar{\tau}_j, \text{value}_j)$ indicates that the value in the time interval $\bar{\tau}_j = [\tau_{j_s}, \tau_{j_e}]$ is value_j , for $1 \leq j \leq n$. $\bar{\tau}_1, \dots, \bar{\tau}_n$ are ascending time intervals without overlap, satisfying $\tau_{j_s} < \tau_{j_e} \leq \tau_{j+1_s}$, for $1 \leq j < n$. Note that τ_{n_e} can be *Now*, which means that the value at any time after τ_{n_s} is value_n . For example, the “status” temporal property of the road in Fig. 1 can be represented by a *Time Interval Series* $\Psi = \langle ([“8:00”, “8:15”), “slow”), ([“8:15”, “8:20”), “jam”), ([“8:20”, “8:45”), “smooth”), ([“8:45”, Now), “slow”) \rangle$.

The *Time Interval Series* extends the commonly used concepts of “Time Series [32]” and “Time Sequences [33]” that are typically defined as a set of tuples $\langle v, t \rangle$, where v represents a data object and t represents a time point signifying when the data object changes [32]. By replacing the time point τ with a time interval $\bar{\tau}$ in each tuple, users can directly define the value of a time interval $\bar{\tau}$ rather than specifying the value on every chronon τ satisfying $\bar{\tau}_s \leq \tau < \bar{\tau}_e$.

The *Time Interval Series* utilizes the “Point-based semantics” [34], [35], meaning the data can be interpreted as a sequence of states indexed by points in time (i.e., Chronons). This indicates that the decomposition of time intervals into chronons does not affect the semantics of data [35] (and vice versa). For example, $\langle ([1, 4), v) \rangle$ are semantically equal to $\langle (1, v), (2, v), (3, v) \rangle$ (if the duration of a chronon is 1). If the time intervals of two adjacent tuples are continuous and their values are identical, say $\Psi_1 = \langle ([\tau_a, \tau_b), v), ([\tau_c, \tau_d), v) \rangle$ and $\tau_b = \tau_c$, then Ψ_1 are considered semantically equivalent to a coalesced *Time Interval Series* $\Psi_2 = \langle ([\tau_a, \tau_d), v) \rangle = \Psi_1$. Based on this semantics, redundant tuples in the *Time Interval Series* can be coalesced naturally to save space, particularly when value changes in PETG data occur less frequently than event updates. This scenario is common when updates in PETG data are automatically generated by IoT sensors at regular intervals.

Definition 4 (Temporal property graph): A temporal property graph is defined as $TG = (V, E)$. V is a set of vertices $v = (vid, L, P, TP)$, where vid is the identifier of vertex v , which uniquely determines v in V ; L is the set of label l marking v ; P is the set of (non-temporal) property $p = (name, value)$ of v where $name$ is the name of the property and $value$ is the property value; TP is the set of temporal properties $tp = (name, \Psi)$ of v where Ψ is a *Time Interval*

Series. E is the set of edges $e = (eid, v_s, v_e, L, P, TP)$, where eid is the identifier of e ; v_s is the starting vertex of e ; v_e is the end vertex of e ; L is the label set of e , P and TP are the non-temporal and temporal property sets of e respectively. Multiple edges are allowed between two vertices.

Notes that: (1) Topological changes in a temporal graph can also be modeled by adding a temporal property to the vertices/edges representing their valid time. (2) Different temporal properties can have chronons with different durations. For example, a “travel-time” temporal property of an edge (representing a road) may use chronons whose duration is a minute. But a “passable” temporal property on the edge may use chronons whose duration is an hour.

B. Operators of Temporal Property Graph

We define a set of basic operators for the temporal property graph model in Table II. Based on their operational targets, operators are categorized into five groups: (1) Topology, (2) Non-Temporal Property, (3) Temporal Property, (4) *Time Interval Series*, and (5) Time Interval. The operators in the “Topology” and “Non-temporal property” categories are the same as the operators in the property graph model [36], providing backward compatibility. Operators in the other categories are newly added to handle reads and writes of temporal properties and related *Time Interval Series* and time intervals.

We next briefly introduce two fundamental operators, i.e., *setTP()* and *getTP()*. Operator *setTP()* allows updating the *Time Interval Series* of a temporal property and guarantees the “Point-based Semantics” [35] of the *Time Interval Series*. Operator *getTP()* retrieves a *Time Interval Series* slice from the specified temporal property. The slice of *Time Interval Series* can be further accessed as an ordered list of $(\bar{\tau}, v)$ triples by *entry()*. So in the example of traffic temporal graph data (Fig. 1), after invoking *setTP(road, “status”, “08:18”, Now, “jam”)*, the call of operator *getTP(road, “status”, “08:10”, Now)* would return a *Time Interval Series* $\Psi = \langle ([“08:10”, “08:15”), “slow”), ([“08:15”, Now), “jam”) \rangle$.

C. Queries of Temporal Property Graph

Using the temporal property graph operators, we can implement more complex operations on PETG data. The following are some common temporal graph operations (also used in our experimental study), building on these operators:

- (1) *Update* sets the value of tp on entity $v|r$ during $\bar{\tau}$ to v , i.e., a single *setTP()* operation.
- (2) *Append* is a sequence of *setTP()* operations on tp of an entity $v|r$, i.e., $[setTP(v|r, tp, \bar{\tau}_1, val_1), \dots, setTP(v|r, tp, \bar{\tau}_n, val_n)]$, satisfying $\bar{\tau}_i \cap \bar{\tau}_{i+1} = \emptyset$ and $\tau_{i_s} < \tau_{i+1_s}$ for $1 \leq i < n$. Additionally, if Ψ of the property on the entity is not an empty set, *Append* should also satisfy $\tau_{max} < \tau_{1_s}$ where τ_{max} is the latest non *NOW* chronon in Ψ .
- (3) *Entity-History* queries the history of tp on an entity $v|r$ during $\bar{\tau}$, i.e., a single *getTP()* operation.
- (4) *Snapshot* queries the values of tp on all entities in a graph at a specified chronon τ , implemented by iterating all entities and calling the *getTP(e, tp, τ)* on each entity.

TABLE II
OPERATORS OF TEMPORAL PROPERTY GRAPH

Operation Target	Operators Definition	Description
Topology	$newNode(l_0, l_1, \dots) \Rightarrow v$	create a vertex v with labels l_0, l_1, \dots marking it
	$newRel(v_s, v_d, l_0, l_1, \dots) \Rightarrow r$	create an edge r from v_s to v_d with labels
	$getNode(l_0, l_1, \dots) \Rightarrow [v, \dots]$	return all vertices whose labels matching l_0, l_1, \dots
	$getRel(v, l_0, l_1, \dots) \Rightarrow [r, \dots]$	return all edges of v whose labels matching l_0, l_1, \dots
	$getStart(r) \Rightarrow v_s$	return r start node v_s
	$getEnd(r) \Rightarrow v_d$	return r end node v_d
	$delNode(v)$	delete v and its connected edges
Non-temporal Property	$delRel(v_s, v_d, l_0, l_1, \dots)$	delete all edges from v_s to v_d whose labels matching l_0, l_1, \dots
	$setProp(v r, p, val)$	set v (or r)'s non-temporal property p 's value to val
	$getProp(v r, p) \Rightarrow val$	return v (or r)'s non-temporal property p 's value
Temporal Property	$rmProp(v r, p)$	delete the non-temporal property p on v (or r)
	$setTP(v r, tp, \bar{\tau}, val)$	set v (or r)'s temporal property tp 's value to val during $\bar{\tau}$
	$getTP(v r, tp, \bar{\tau}) \Rightarrow \Psi$	return v (or r)'s temporal property tp 's Time Interval Series Ψ during $\bar{\tau}$
Time Interval Series	$rmProp(v r, tp)$	delete the temporal property tp on v (or r)
	$slice(\Psi, \bar{\tau}) \Rightarrow \Psi_{sub}$	return a truncate Time Interval Series whose time within $\bar{\tau}$
	$valueAt(\Psi, \tau) \Rightarrow value$	return the value of Ψ at time τ
	$valueList(\Psi, \bar{\tau}) \Rightarrow [value, \dots]$	return the value list of Ψ during $\bar{\tau}$
Time Interval	$set(\Psi, \bar{\tau}, val) \Rightarrow \Psi_{new}$	change Ψ value to val during $\bar{\tau}$
	$entry(\Psi) \Rightarrow [(\bar{\tau}_{slice}, val), \dots]$	access Ψ as a list of $(\bar{\tau}_{slice}, val)$ entries
	$intersection(\bar{\tau}_1, \bar{\tau}_2, \dots, \bar{\tau}_n) \Rightarrow \bar{\tau}_{new}$	returns the intersection of two or more time intervals (brief as \cap)
	$union(\bar{\tau}_1, \bar{\tau}_2, \dots, \bar{\tau}_n) \Rightarrow \bar{\tau}_{new}$	returns a time interval of multiple continuous time intervals (brief as \cup)
Time Interval	$diff(\bar{\tau}_1, \bar{\tau}_2) \Rightarrow \bar{\tau}_{new}$	return the difference of two time intervals
	$shift(\bar{\tau}_{old}, \tau) \Rightarrow \bar{\tau}_{new}$	move the start point of $\bar{\tau}_{old}$ to τ without duration change

Algorithm 1: *ReachableArea*(TG, v_s, τ_s, dur)

Output: Γ (earliest arrival time of nodes that are reachable from v_s within dur departing at τ_s).

```

1  $\Omega \leftarrow \emptyset; \Delta \leftarrow \emptyset; \Gamma \leftarrow \emptyset;$  // Init
2  $\Omega \leftarrow \Omega \cup v_s; \Gamma[v_s] \leftarrow \tau_s; \tau_{max} \leftarrow \tau_s + dur$ 
3 while  $\Omega \neq \emptyset$  do
4    $v_n \leftarrow \text{earliestArriveNode}(\Omega, \Gamma)$ 
5    $\Omega \leftarrow \Omega - v_n; \Delta \leftarrow \Delta \cup v_n$ 
6   if  $\Gamma[v_n] < \tau_{max}$  then
7     foreach  $r \leftarrow \text{getRel}(v_n, \text{outgoing})$  do
8        $v \leftarrow \text{getEnd}(r)$ 
9       if  $v \in \Omega$  then
10          $\tau_v \leftarrow \text{earliestArrTime}(r, \Gamma[v_n], \tau_{max})$ 
11         if  $\tau_v < \Gamma[v]$  then  $\Gamma[v] \leftarrow \tau_v$ 
12       else if  $v \notin \Delta$  then
13          $\tau_v \leftarrow \text{earliestArrTime}(r, \Gamma[v_n], \tau_{max})$ 
14          $\Omega \leftarrow \Omega \cup v; \Gamma[v] \leftarrow \tau_v$ 
15 Function  $\text{earliestArrTime}(r, \tau_0, \tau_1):$ 
16    $arriveT \leftarrow \tau_1$ 
17    $\Psi \leftarrow \text{getTP}(r, \text{"travel time"}, [\tau_0, \tau_1])$ 
18   foreach  $([\tau_a, \tau_b], val) \leftarrow \text{entry}(\Psi)$  do
19      $arriveT \leftarrow \min(arriveT, \tau_a + val)$ 
20 return  $arriveT$ 

```

(5) *Graph Aggregate Temporal Property (GATP)* performs aggregation $f(\Psi)$ on all entities in the graph, where *time interval series* Ψ is the result of query $\text{getTp}(v|r, tp, \bar{\tau})$ on each entity of tp during $\bar{\tau}$. The aggregate function f can be “min”, “max”, “avg” or user-defined aggregation functions.

(6) *Entity Temporal Property Condition (ETPC)* queries entities (nodes or edges) whose value of temporal property tp is within the specified value ranges $[v_{min}, v_{max}]$ during specified time interval $\bar{\tau}$.

(7) *Reachable Area* returns all nodes $v \in V$ (and their earliest

arrival time $\Gamma[v]$) that can be reached ($v \in \Gamma$) within a given time duration dur , departing from a specific node v_s at a given time τ_s . Algorithm 1 shows an implementation of the calculation process of a reachable area query using the temporal property graph model and its operators. The process is delivered from the earliest arrival path algorithm for the temporal road graph [37]. The earliest arrival time of road r is calculated by querying its “travel time”, which is a function of departure time τ_0 . The function is packed by a *Time Interval Series* Ψ fetched by $\text{getTp}()$. The $\text{earliestArriveNode}()$ returns a node $v_n \in \Omega$ whose arrival time is earliest according to Γ (not defined in the code because it does not contain operators of the temporal property graph).

D. Temporal Query Language

We develop a high-level query language, named TCypher, to support temporal property graph queries. TCypher is extended from *Cypher* [36], a popular declarative query language of graph databases. We try to minimize the modifications so users familiar with Cypher can easily use TCypher to manipulate temporal graphs. Table III are some example statements of TCypher with respect to the queries of Section III-C.

TCypher mainly expands upon Cypher in two ways: (1) It introduces two new basic data types for describing Time Intervals and *Time Interval Series*. For example, *Time Interval Series* can be used as property values when defining properties (*TIS* expression in statement (i), Table III). (2) It incorporates many functions that manipulate *Time Interval Series* and construct predicates (*TIS_WITHIN* expression in statement (iii), Table III) for querying temporal properties in a temporal graph. Note that TCypher also supports user-defined functions (UDF), allowing complex queries to be implemented as functions that can be called in the TCypher language.

TABLE III
TCYPER EXAMPLE QUERIES MANAGING A TRAFFIC GRAPH

```
#Statement (i) Update a temporal property
MATCH ()-[road {name: "Haidian East Road"}]->() SET
road.travel_time = TIS("2010-05-01 08:00" -- "2010-05-01
08:10": 36)
#Statement (ii) GATP(MAX) Query
MATCH ()-[road]->() RETURN road.name, TIS_AGGR_MAX(road
.travel_time, "2010-05-01 08:00" -- "2010-05-01 08:30")
#Statement (iii) ETPC Query
MATCH ()-[road]->() WHERE TIS_WITHIN(road.travel_time,
'2010-05-01 08:00' -- '2010-05-01 08:30', 600, 1200)
RETURN road.name
```

IV. SYSTEM DESIGN

This section presents the design of PETGraphDB.

A. Design Goals and Principles

PETGraphDB is a single-machine PETG data management system with the following design goals and principles.

(1) *Native support for valid-time temporal property graph model.* PETGraphDB natively supports the temporal property graph model, providing an intuitive, flexible, and effective way to operate PETG data. The valid time of data is specified by users, allowing for modification and analysis of existing data.

(2) *ACID properties and high HTAP transaction throughput.* PETGraphDB should support user-level transactions. Moreover, PETGraphDB should support a time-related concurrency control mechanism to improve transaction throughput.

(3) *Compatibility with current graph databases.* PETGraphDB should provide (API and file format) compatibility with Neo4j, the most popular graph data management system. This implies PETGraphDB is also capable of managing the (non-temporal) graph databases created by Neo4j. When the recording of graph dynamics becomes a user requirement, the DBMS running on the database can be transitioned from Neo4j to PETGraphDB seamlessly. This compatibility plays a crucial role in reducing user expenses.

(4) *Space/time efficient storage for frequent Append write and Entity-History query.* PETGraphDB should employ techniques to reduce data redundancy and support efficient *Entity-History* and *Append* write, which are the most frequent read/write queries of PETG data.

(5) *Easy of use.* PETGraphDB should support a high-level declarative query language to facilitate users in developing complex temporal graph queries.

B. Architecture

PETGraphDB extends the architecture of Neo4j to maintain compatibility with current graph databases. The architecture of PETGraphDB is illustrated in Fig. 2. Dedicated temporal property modules (indicated by green cross-hatches) are introduced, while several legacy Neo4j modules (shown with blue hatches) are refactored to incorporate valid-time temporal graph access capabilities. Remaining modules (marked with orange dashed lines) are kept unchanged.

PETGraphDB consists of two main components: the *database kernel* and the *query language processor*. The

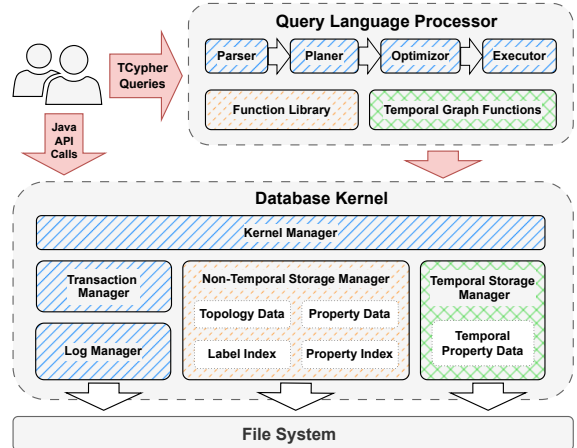


Fig. 2. System architecture of PETGraphDB

database kernel provides comprehensive temporal graph data management and transactional capabilities that are operable through Java APIs. The query language processor is an optional component. When loaded, the system can handle TCypher queries, compiling them into Java procedures and calling the database kernel for execution.

1) *Database kernel:* It implements the data access interface defined in Section III-B and other transaction management interfaces as Java APIs for users to operate the database. It contains five modules: (1) the kernel manager acts as a query portal and manages important control flows in the database; (2) the non-temporal storage manager manages graph topology, non-temporal property data and its indexes; (3) the temporal storage manager manages temporal property data; (4) the transaction manager provides a locking mechanism and private memory buffers for implementing the ACID properties of the database; and (5) the log manager controls transaction logging and fault recovery abilities.

The kernel manager is the core part of the database kernel. It uniformly manages all requests that read, write, and manage the database instance, oversees all internal states of the database instance, and controls all processes across modules. It invokes functionalities from other modules to ensure the ACID properties of database access.

The storage manager manages graph topology data, non-temporal property data, and temporal property data. The temporal and non-temporal properties share the same namespace. The temporal property data module, primary storage of temporal property data, supports efficient *Entity-History* query and *Append* write, which are the most frequent read/write queries of PETG data. The module also minimizes the space cost by eliminating data redundancy.

The transaction manager and the log manager work together to ensure the system's ACID properties and support log-based fault recovery. We also extend the transaction manager to support more efficient concurrent queries of temporal graphs by refactoring its locking mechanism, which allows fine-granularity locks to be added at specified time intervals.

2) *Query language processor*: It is an optional module of PETGraphDB that generates query plans of TCypher queries and compiles them into Java procedures that internally invoke the database kernel and then execute the procedures. To this end, we extend the query parser and function library of the original Cypher language to support TCypher's syntax and semantics, and implement temporal-property-related query operators in the execution engine.

C. Temporal Property Storage

The primary design goals of the temporal property data storage module of PETGraphDB are: (1) efficient handling of the *Entity-History* query (see Section III-C) that examines the historical changes of a known property on a certain node/edge over a specified period of time; (2) accommodating fast data writes, especially the *Append* writing of temporal properties for each node/edge, and (3) reducing disk space usage. In the following discussion, we assume the data items of temporal property storage are in the form of $\langle e, tp, \bar{\tau}, v \rangle$, where e is a vertex/edge, tp is a temporal property, $\bar{\tau} = [\tau_s, \tau_e]$ represents the valid time interval of the data item, and v is the corresponding value during $\bar{\tau}$.

There has been works [38], [39] on access structures of time interval data, but they are less efficient for the Entity-History query, as their query predicates do not contain the entity as a query parameter, with which the non-temporal access structures (such as B-Tree [40] or LSM-Tree [41]) can be used to efficiently answer the Entity-History query by ordering data by $\langle e, tp, \tau_s \rangle$. B-Tree [40] and LSM-Tree [41] provide $O(\log(N))$ complexity when querying from N data items. Moreover, LSM-Tree [41] utilizes the sequential write features of disks for high writing throughput and is capable of handling write-intensive workloads like *Append* in PETG.

However, data skew in the PETG data on the property and time dimension is not considered in LSM-Tree [41]. Properties with low update frequency have fewer records and are sparse in all temporal property data, resulting in inefficient access and difficulties in compressing the data. In addition, the frequently updated recent data can have a smaller file size (or more levels), trading off read efficiency for write performance. Therefore, we designed a tree-based data structure called “Temporal Interval Merge Tree (TIM-Tree)” that drew on the idea of LSM-Tree [41] but introduced extra partition mechanisms in the property and time dimension.

1) *TIM-Tree Data Structure*: Fig. 3 shows the data structure of TIM-Tree. The data items of the TIM-Tree are first partitioned/ordered by tp (square nodes with dots) and then by $\bar{\tau}$ (circle nodes). This method efficiently narrows the search space based on the specified properties and time intervals. Data items inside the partition are then grouped as *Time Span Chunks* (dashed-line boxes). *Time Span Chunks* of a temporal property divide the data into a series of across a series of disjoint, ordered, and contiguous time ranges along the timeline. The chunk size decreases as time increases (a tunable parameter specified by the user) in most cases, which tends to store the most recent data, typically updated more frequently,

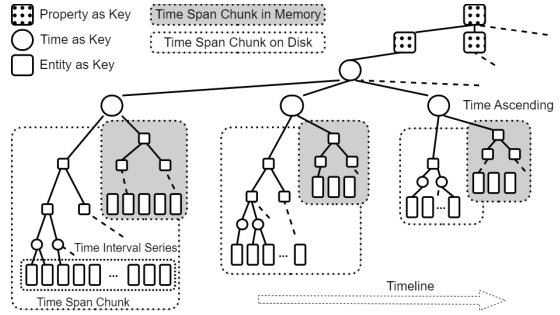


Fig. 3. The structure of Time Interval Merge Tree

in smaller chunks. The nodes in the upper levels of the TIM-Tree, which index *Time Span Chunks* by tp and $\bar{\tau}$, are stored in memory, reducing the overhead of disk I/O operations during the initial search phase and allowing for quick filtering based on these primary dimensions. Inside the *Time Span Chunks*, data items are of a single property and a range of time; they are ordered by $\langle e, \tau_s \rangle$ in ascending order and can be interpreted as an ordered set of *Time Interval Series* (rectangles grouping leaf nodes) for each e . A *Time Span Chunk* can be stored either on disk or in memory (dashed-line boxes with gray background); the latter corresponds to their counterparts on disk (sibling dashed-line boxes with white background) and are used in updating the TIM-Tree. Each in-memory *Time Span Chunk* and its counterpart chunk on disk share the same property and time range; they correspond to the in-memory component and disk component of the LSM-Tree [41].

2) *Data Items coalescing and splitting*: Based on the “Point-based semantics” [35] of the *Time Interval Series*, multiple data items $\langle e, tp, \bar{\tau}_0, v \rangle \dots \langle e, tp, \bar{\tau}_k, v \rangle$ can be merged (coalesced) into a single data item $\langle e, tp, \bar{\tau}, v \rangle$ if they are in the same *Time Span Chunk* and have continuous $\bar{\tau}_i$ for $0 \leq i \leq k$. The coalesced data item has a larger time interval $\bar{\tau} = \text{union}(\bar{\tau}_0, \dots, \bar{\tau}_k)$. This reduces the storage overhead. On the other hand, if a data item’s $\bar{\tau}$ spans across multiple *Time Span Chunks*, then it can be split into multiple data items $\langle e, tp, \bar{\tau}_i, v \rangle$ whose $\bar{\tau}_i$ are coalesced to the time interval of the corresponding *Time Span Chunks*.

3) *Updating the TIM-Tree*: Updates of TIM-Tree arrive in the form of $\langle e, tp, \bar{\tau}, v \rangle$. These updates are firstly applied to the in-memory components (*Time Span Chunks*) according to their tp and $\bar{\tau}$ (may be split). When an in-memory component reaches a fixed size threshold, it triggers a compaction between disk and memory components, producing a new disk component with merged data and clearing the memory. The new disk component is flushed to disk with bulk sequential writes (rather than random I/O), which improves the overall write efficiency for handling *Append* write in PETG. The merge process adopts the merge-sort algorithm [42] whose time complexity is $O(N + m)$ where N and m are the number of data items in the disk and corresponding in-memory component. Additionally, a background process merges small, adjacent *Time Span Chunks* on disk with their in-memory counterparts, achieving the TIM-Tree feature that recent chunks remain small and older ones grow larger.

4) *Querying the TIM-Tree*: An Entity-History query $getTP(e^q, tp^q, \bar{\tau}^q = [\tau_s^q, \tau_e^q])$ is answered by: (1) Binary-searching the in-memory catalogue to locate the *Time Span Chunks* (both on-disk and in-memory) that intersect tp^q and $\bar{\tau}^q$. (2) Within each candidate chunk, locating the first data item satisfying $e = e^q$ and $\tau_s \leq \tau_s^q$ (via binary search). (3) Sequentially scanning the next item until $\tau_s \geq \tau_e^q$ or $e \neq e^q$, getting a items. (4) Combining the results from on-disk *Time Span Chunks* with those from their in-memory counterparts. Data items from in-memory components take precedence because they are more recently updated. Since the data volume of an in-memory component is limited and relatively small, this merging step requires only $O(1)$ time. The overall time complexity is $O(\log(n) + a)$ where n is the total number of items for the temporal property and a is the size of the result set in step (3). This approach ensures high performance for Entity-History queries.

D. Transaction Management and Fault Recovery

The design goal of transaction management and fault recovery in PETGraphDB is to ensure the ACID properties of PETG data processing while also providing high transaction performance. However, the transaction mechanism of Neo4j falls short of achieving these objectives once temporal property storage is introduced. To address these issues, PETGraphDB extensively refactors the transaction and logging modules of Neo4j. These modules are modified to accommodate the management of temporal property data and are enhanced with a more efficient fine-grained multi-level locking mechanism.

The transaction manager of PETGraphDB ensures the ACID properties of the access to temporal graph data. The manager runs in two modes: original mode and temporal mode. When handling transactions involving no temporal property, the transaction manager runs in its original mode, which falls back to Neo4j's transaction mechanism. When handling transactions involving temporal property, the transaction manager would upgrade to its temporal mode, which not only includes all features of the original mode, but also plugins new functions: (1) allocate an in-memory data structure as the transaction's private variable which accepts updates of temporal properties, and (2) create new types of log entries that represent temporal property updates and record them in Neo4j's log. The new functions integrate temporal graph data with Neo4j's transaction management and fault recovery system, ensuring the ACID properties of PETGraphDB are fully supported by the modified transaction engine.

The fine-granularity multi-level locking mechanism is designed and added to the temporal mode of the transaction manager to improve the concurrency performance of the system by reducing conflicts in typical PETG workloads. Empirical analyses of PETG data and their access patterns show that most requests are limited to specific time intervals and involve only a subset of nodes and edges. However, the current entity-level locking mechanism in Neo4j leads to unnecessary waiting for requests that access disjoint time intervals on the same node or edge, which results in poor

TABLE IV
MUTUAL EXCLUSION LOCKS IN PETGraphDB

$L^S(e)$	$L^X(e)$	$L^S(e, tp, \bar{\tau}_a)$	$L^X(e, tp, \bar{\tau}_a)$
$L^S(e)$		×	
$L^X(e)$	×	×	×
$L^S(e, tp, \bar{\tau}_b)$		×	× iff $\bar{\tau}_a \cap \bar{\tau}_b \neq \emptyset$
$L^X(e, tp, \bar{\tau}_b)$		×	× iff $\bar{\tau}_a \cap \bar{\tau}_b \neq \emptyset$

concurrency performance. To address this issue, we designed a fine-grained multi-level locking mechanism that supports more precise locks and eliminates unnecessary waiting, thus improving overall performance.

Table IV illustrates the mutual exclusion of the lock mechanism (× denotes a conflict). $L^S(e)$ and $L^X(e)$ are locks at the entity-level on entity e (a node or relationship) and all its properties, where $L^S(e)$ is a shared lock and $L^X(e)$ is an exclusive lock. $L^S(e, tp, \bar{\tau})$ and $L^X(e, tp, \bar{\tau})$ are locks at the property-level that can be specific to a particular time interval $\bar{\tau}$ within the temporal property tp of a given entity e . By reducing the granularity of locks, we decrease the probability of request conflicts, thereby improving concurrency performance.

V. IMPLEMENTATION

This section provides details on the implementation of PETGraphDB, including temporal property storage, transaction management and fault recovery.

A. Temporal Property Storage

This section presents the implementation of the TIM-Tree, describing its data organization, batch write process, file merge strategy, and data redundancy reduction mechanism.

1) *Data organization*: PETGraphDB implements the TIM-Tree as shown in Fig. 4. The upper-level nodes of the TIM-Tree are stored in the Metadata File and loaded into memory at system startup. *Time Span Chunks* on disk are implemented as a series of Stable/Unstable Files, and their in-memory counterparts are implemented as Local Memtables. Disk data files utilize SSTables [43], which contain ordered key-value pairs in data blocks and key range indices. The Global Memtable (default 64MB, user-configurable), which acts as a write buffer size controller, delegates all updates to Local Memtables. The Buffer Files serve as backups for Local Memtables during transaction checkpoint events.

2) *Batch write*: To minimize the I/O cost of reordering data when modifying disk data, we adapt an “export/merge” approach. Changes are first written to the Global Memtable, while a background service periodically merges this data with disk data using the merge-sort algorithm [42] and flush it to the disk in a batch manner. Specifically, the service (1) activates when the Global Memtable reaches a set size; (2) allocates updates whose start times before the maximum end time of Stable/Unstable Files to Local Memtables; (3) merges full Local Memtables (default 10MB, user-configurable) to their corresponding Stable/Unstable Files; and (4) packages any remaining updates into a new Unstable File of level 0.

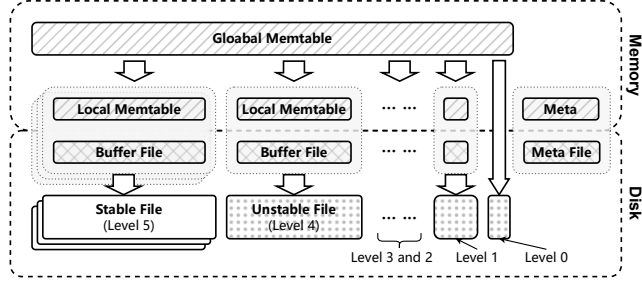


Fig. 4. Data organization of temporal property storage

3) *File merge strategy*: To reduce frequent I/O from small files, a file merge strategy is used. This strategy introduces levels from 0 to 5 to limit unnecessary merging of aged data. Level 5 files are Stable Files with the largest sizes, while Level 0 files are the smallest. Each temporal property can have multiple Level 5 Stable Files and at most one Unstable File in levels 0 to 4. After generating a level 0 Unstable File, an extra process checks for existing level n Unstable Files. If another exists, the two files are merged, producing a level n+1 Unstable File (or a Stable File at level 5), and the check is repeated. This strategy maintains the TIM-Tree feature, ensuring smaller recent chunks and larger older ones.

4) *Data redundancy reduction*: To reduce disk data size, we develop three mechanisms: (1) When storing continuously changing property values, we store the data item as $\langle e, tp, \tau_s, v \rangle$ instead of $\langle e, tp, \tau_s, \tau_e, v \rangle$, as τ_e can be calculated from the time of the next preceding data item. This design effectively reduces the disk space usage because most state changes in PETG data occur continuously, allowing us to save space by only storing τ_s . Furthermore, since data items are sorted in ascending order by $\langle e, \tau_s \rangle$ within each file, calculating τ_e becomes straightforward by accessing the next data item. (2) When a data item's time interval spans multiple files, it is divided into several files for storage. This can be thought of as having a “checkpoint” in each disk file. The proportion of stored “checkpoint” information to total file data decreases as the size of files increases, which is adjustable through the Global Memtable size set by users. (3) Each data block stored in disk files undergoes prefix compression using the Snappy algorithm [44]. Since data items in disk files are ordered, there is a high probability of redundancy between adjacent data items, such as identical or similar ids of e and shared high-order bits in τ_s .

B. Transaction Management and Fault Recovery

In this section, we elaborate on PETGraphDB’s transaction management and fault recovery module, which extends Neo4j’s native mechanisms while still delegating core ACID guarantees to Neo4j’s original engine.

Neo4j’s ACID guarantees rest on an in-memory transaction buffer: all writes are staged per transaction and flushed to storage only on successful commit, otherwise discarded, ensuring atomicity and consistency; a write-ahead log (WAL) secures durability, while entity-level locks acquired during updates and released on commit/rollback enforce isolation.

TABLE V
CHARACTERISTIC/STATISTICS OF DATASETS

Dataset	Energy	Traffic	SYN
Raw data size	3.7GB	41GB	106GB
Time span	2012-2014	2010.5-11	1-1B
# static vertices	1.5K	80K	400K
# static edges	2.2K	110K	10M
# events (vertices property update)	39M	-	2B
# events (edges property update)	-	1.39B	2B
# temporal properties	V9, E0	V0, E3	V3, E1
Temporal property non-redundancy	V0.8 E-	V- E0.4	V0.3 E0.5

PETGraphDB extends Neo4j’s transaction pipeline at three points. Within the in-memory stage, it introduces (i) a structure for temporal data in the transaction buffer, (ii) user-level temporal-graph APIs that inject request data into the buffer, and (iii) a flush routine that writes temporal data from the buffer to storage, leaving Neo4j’s original commit/abort logic intact to guarantee atomicity and consistency. Within the logging stage: it adds (i) new WAL entry types for temporal data, (ii) a buffer→WAL writer, and (iii) a WAL→storage flusher for crash recovery, all executed under Neo4j’s native logging and recovery mechanisms to ensure durability. Within the lock-acquiring stage, it employs a fine-granularity multi-level locking mechanism, which acquires an entity-level shared lock first, then a fine-grained temporal exclusive lock for the relevant time interval on write. This eliminates gratuitous waits and improves transaction efficiency. In addition, the fine-grained locks employ Neo4j’s lock and deadlock detection logic in isolated memory, ensuring the correctness of native and temporal locking mechanisms.

VI. EXPERIMENTAL STUDY

This section evaluate the performance of PETGraphDB in typical PETG data management scenarios from three aspects: utilization of disk space, latency of read and write operations, and throughput of concurrent transactions.

A. Experimental Setup

1) *Datasets*: Three datasets are used for the evaluation (two real-world temporal graph datasets and a synthetic temporal graph data): (1) Traffic, traffic data of Beijing [9], (2) Energy, data from European renewable energy power system [11], and (3) SYN, data generated by a temporal graph data generator. Some statistical indicators of the datasets are listed in Table V. The “temporal property non-redundancy” is the average probability that update events of temporal properties in a dataset lead to value changes (“V” for temporal properties on nodes, “E” for those on edges). This metric characterizes how much data can be considered semantically non-redundant.

2) *Baseline systems*: We compared PETGraphDB (referred to as PETG) with relational databases (PostgreSQL 17.5, referred to as PG), temporal relational databases (MariaDB 11.4.7, referred to as MA), and graph databases (Neo4j 4.4.37, referred to as Neo). These databases were chosen because they support user-level transactions, a valid-time data model,

TABLE VI
DETAILS OF STORAGE SPACE USAGE OF EACH SYSTEM (BYTES)

Metrics\Systems	Datasets				Traffic				SYN			
	PETG	PG	MA	Neo	PETG	PG	MA	Neo	PETG	PG	MA	Neo
Static Data	2544K	568K	496K	2528K	38.3M	29.0M	25.6M	39.2M	1490M	1111M	996M	1616M
Temporal Data	3.17G	4.25G	4.75G	8.09G	14.5G	119G	133G	172G	41.3G	327G	365G	416G
Total Size	3.17G	4.25G	4.75G	8.10G	14.6G	119G	133G	172G	42.8G	328G	366G	417G
Raw Data Size				3.69G			41.1G				106G	
Amplification ratio	0.859	1.15	1.29	2.20	0.355	2.90	3.24	4.18	0.404	3.09	3.45	3.93

and are currently common solutions for temporal graph data management. Other temporal graph systems are not considered because they only natively support temporal graph data with transaction-time [18], [19] or do not support full user-level transactions [12], [13], [20]–[25].

3) *Applications and Configurations*: We implement applications on both PETGraphDB and the baseline systems. These applications support typical queries of PETG data (see Section III-C), including four read operations: *Entity-History*, *Snapshot*, *GATP (max)*, and *ETPC*; two write operations: *Append* and *Update*; and a temporal graph analytical query *Reachable Area* (only available on the Traffic dataset).

When loading data on Neo4j, we create nodes that represent a time interval and link these nodes with entities in the temporal graph [15]. For PostgreSQL, we create a table to store the nodes with their static properties and a table to store the relationships with their static properties. The temporal properties of nodes/rels are stored in corresponding tables in the form of $\langle e, \tau_s, v_{tp_1}, \dots, v_{tp_n} \rangle$. For MariaDB, valid-time temporal tables are used to store the temporal property data in the form of $\langle e, \tau_s, \tau_e, v_{tp_1}, \dots, v_{tp_n} \rangle$. Note that for PostgreSQL and MariaDB, indexes on $\langle e, \tau_s \rangle$ are created to accelerate the *Entity-History* query.

The experiments are carried out on a Dell T630 workstation with Intel Xeon(R) CPU E5-2640v3@2.60GHz (x2, 16/32 physical/logical cores) and 192GB memory, with a storage of Dell PERC H730 Adp RAID1 disk array (SAS 7200 rpm, 8TB). The operating system is Ubuntu 24.04.2 LTS, with OpenJDK (version 11.0.27+6) installed. For PETGraphDB and each baseline system, we allocate 48GB memory ($Xmx=48g$ for systems based on JVM) and use the “read-committed” isolation level for transactions by default.

B. Space Usage

To demonstrate the space efficiency of PETGraphDB, we analyze the space usage of PETGraphDB and the baseline systems, store the full datasets Energy, Traffic, and SYN on them, and check their disk space usage (excluding transaction logs). The results are shown in Fig. 5 and Table VI.

PETGraphDB takes up the least storage space (on average 33% of PostgreSQL, the current best solution) and has more advantages (12.6% and 13.1% of PostgreSQL) on the Traffic and SYN datasets, whose non-redundancy ratio is lower than the Energy dataset. This shows the power of PETGraphDB’s space-saving abilities in data model and temporal property storage. Table VI lists the details of storage space usage, from

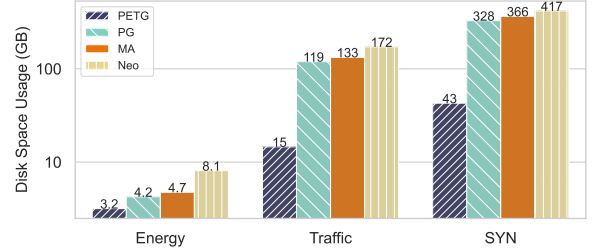


Fig. 5. Evaluation of database disk space usage (GB).

which we can see the majority of space is occupied by the temporal parts of PETG data, whose space-saving strategies decide the final space cost. The storage amplification ratio (database space cost to raw data size) is 66.7% smaller than PostgreSQL on average (25.3%, 87.7% and 87.1% in these datasets, respectively). It is worth to point out that the storage space of PETGraphDB is even smaller than the raw data size, its storage amplification ratio is approximately the same as the datasets’ temporal property non-redundancy rate (0.859 vs 0.8 in Energy, 0.355 vs 0.4 in Traffic, 0.404 vs 0.4 in SYN), which indicates that the temporal property storage effectively eliminates redundant information in the temporal data.

C. Latency

1) *Latency of read and write operations*: To test the latency of PETGraphDB, we evaluate the response time of read and write operations of PETGraphDB and the baseline systems with seven typical operations defined in Section III-C on three datasets. Each test was performed by randomly generating 10k requests for each type of operation on each dataset. The results are shown in Table VII wherein the numerical value represents the 90% percentile of the response time of these requests, indicating that 90% of the requests can be completed within this time limit. The empty cell “-” represents cases in which the system did not respond to any requests within 1 hour. We find the following:

(1) PETGraphDB exhibits a significant overall advantage on latency compared to the current best system (i.e., PostgreSQL and MariaDB) and has more advantage when the dataset gets larger. The operations are speeding up by 267× on average (85.8×, 117.6×, and 622.9× for datasets Energy, Traffic, and SYN, respectively). Among 19 read/write scenarios, PETGraphDB outperforms the current best system (PostgreSQL and MariaDB) in 18 scenarios, and shows a

TABLE VII

COMPARISON OF REQUESTS LATENCY OF READ AND WRITE OPERATIONS
(MILLISECONDS, 90% PERCENTILE, - FOR TIMEOUT)

Dataset	Operation	PETG	PG	MA	Neo
Energy	Entity-History	2.0	6.0	64	18k
	Update	5.0	2.0k	6.4k	35k
	Append	11	8.0	7.1k	992k
	Snapshot	156	2.6k	76k	18k
	GATP(Max)	159	7.4k	17k	19k
	ETPC	132	6.3k	73k	19k
Traffic	Entity-History	3.0	35	344	1.2m
	Update	5.0	2.3k	21k	-
	Append	6.0	8.0	17k	-
	Snapshot	5.2k	379k	-	1.5m
	GATP(Max)	10k	432k	873k	1.3m
	ETPC	4.6k	335k	-	1.0m
	Reachable Area	695	112k	395k	-
SYN	Entity-History	1.0	44	18k	-
	Update	6.0	21k	901k	-
	Append	7.0	1.3k	101k	-
	Snapshot	553k	2.4m	1.2m	-
	GATP(Max)	443k	2.0m	1.2m	-
	ETPC	394k	1.1m	1.1m	-

performance improvement of 1 or 2 orders of magnitude in 13 of 19 scenarios.

(2) PETGraphDB achieves an average improvement of $19.6\times$ on the Entity-History query. This improvement also scales with dataset size ($3.0\times$, $11.7\times$ and $44\times$ for dataset Energy, Traffic and SYN, respectively). This improvement is due to PETGraphDB's design of TIM-Tree partitioning and sorting of temporal property data by time, while MariaDB and Neo4j can only index either the start or end of time intervals, which only partially accelerates the queries, causing all queries and update operations to involve traversing unnecessary time points. For a temporal property with a total of n data items, PETGraphDB's worst-case complexity of Entity-History query is $O(\log(n))$, while other systems can be $O(n)$. PostgreSQL's performance is closest to that of PETGraphDB, as it uses B-Tree [40] indexes, providing a time complexity of $O(\log(n))$. However, it requires access to both the index file and the data file, while PETGraphDB has internal ordering and does not require extra access to the index.

(3) The latency of the *Update* operation is significantly larger (at least $16.2\times$) than the *Append* operation for PostgreSQL, while they are close (the difference is less than 20 milliseconds) in PETGraphDB. This is because PostgreSQL needs to delete items and insert new ones to correctly execute updates, with every operation introducing the overhead of maintaining the index, while append involves only one insertion with little overhead of index maintenance. PETGraphDB directly inserts data items into memory and writes them to disk in a batch manner, providing an overall efficiency of data write. PETGraphDB is a bit slower than PostgreSQL on the *Append* operation in the Energy dataset because the database for this dataset is small enough to fit into memory and PETGraphDB involves sort commands in the write operation, while PostgreSQL does not.

(4) PETGraphDB shows higher speedup (average $34.2\times$) on

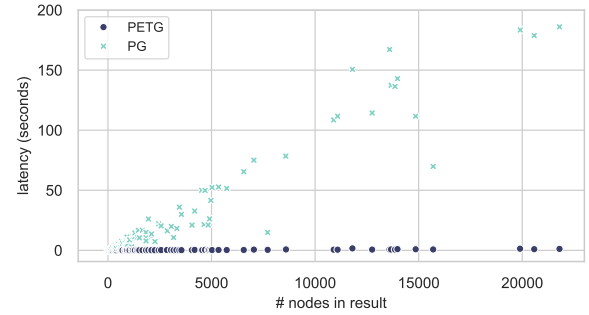


Fig. 6. Latency of Reachable Area query scales with result size (each data point represents a query)

the analytic queries (*Snapshot*, *GATP(max)*, and *ETPC*) than on the Entity-History query (average $19.6\times$). This greater improvement is caused by the data locality of PETGraphDB: data items with a closer time interval (of all entities) are packed in adjacent locations on disk, which is not implemented by baseline systems.

2) *Latency of traversal temporal graphs*: To test the ability of PETGraphDB to simultaneously handle temporal and topological queries, we conduct the following experiment using the *Reachable Area* query (see Algorithm 1) on Traffic, which fetches a sub-temporal-graph whose nodes are reachable within a given time duration departing from the specified node. We generate 100 reachable area queries on the Traffic dataset, randomly selecting a departing node and a maximal travel time range from 120s to 1200s, and track the result size (number of nodes) of the queries. The results are shown in Fig. 6.

(1) The execution latency time scales almost linearly according to the number of nodes in the result sub-temporal-graph.

(2) PETGraphDB is on average $119.38\times$ faster than PostgreSQL (the current fastest solution) in queries whose result has at least two nodes. The latencies of PETGraphDB show a flatter slope, meaning that PETGraphDB gains more advantage when performing larger queries. When fetching a reachable sub-temporal-graph with 19903 nodes, PostgreSQL takes 183.47 seconds, while PETGraphDB only costs 1.373 seconds ($133.6\times$ faster). This advantage is the overall effect of the TIM-Tree data structure of temporal property and the native graph topology implementation of Neo4j. By further extracting the cost of single operators, we observe that TIM-Tree provides a *getTP()* operator whose average cost is

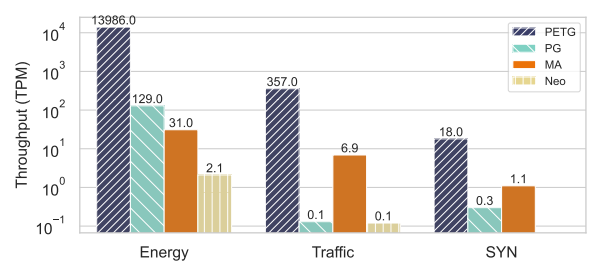


Fig. 7. Evaluation of transaction throughput on HTAP workload

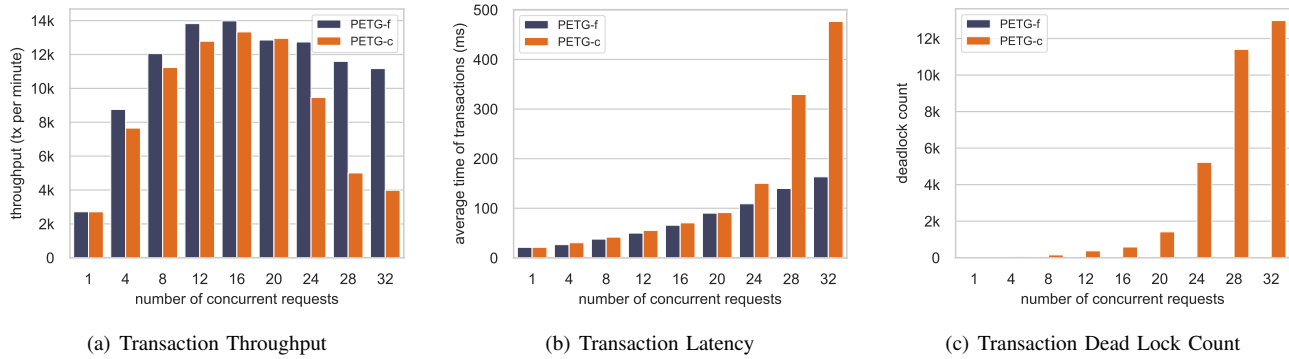


Fig. 8. Effectiveness of fine-granularity multi-level locking mechanism in PETGraphDB

0.26ms (23× faster than PostgreSQL), and the native graph store offers a *getRel()* operator with an average cost of 0.01ms (70× faster).

D. Transaction Throughput

1) *Throughput of HTAP workloads*: To test the transaction throughput of PETGraphDB, we evaluate the concurrency performance of each system with HTAP workloads on three datasets. Each workload is composed of 100k requests of different types with random parameters. The request proportions are: *Append* 40%, *Update* 5%, *Entity-History* 35%, *Snapshot* 5%, *GATP(max)* 5%, *ETPC* 5%, *Reachable* 5%. The maximum number of concurrent connections is set to 16. The results are shown in Fig. 7.

(1) The throughput of PETGraphDB is average 58.8 times higher than the best existing system, i.e., average 108.4×, 51.7× and 16.3× on datasets Energy, Traffic, and SYN, respectively. This is the combined effect of the technicals applied in PETGraphDB, especially the TIM-Tree data structure and the fine-granularity multi-level locking mechanism.

(2) The throughput of PETGraphDB decreases as the dataset size increases. This is because the latency of analytical temporal graph queries (*Snapshot*, *GATP (max)*, and *ETPC*), which access all entities in the graph, is linear with the size of a graph, thus, they cost more time in a larger dataset.

2) *Effectiveness of fine-grained locks*: To validate the fine-granularity multi-level locking mechanism, we compare fine-grained concurrent locks on HTAP workloads using two types of PETGraphDB instances: PETG-c (using coarser granularity locks) and PETG-f (fine-grained locks), comparing their transaction throughput, average latency, and the number of deadlocks on the Energy dataset. When writing temporal properties, PETG-c adds an Exclusive Lock to the corresponding nodes/edges manually, while PETG-f automatically applies a Shared Lock and uses smaller granularity locks for the query time interval. Each transaction retries every 50ms until committed. To achieve measurable conflict rate in the workload, we use Energy dataset whose size is smallest among all datasets. The conflict rate of two transactions in the workload is 2.34% on entity level and 0.000067% considering time intervals on entities. The results are shown in Fig. 8.

(1) The overall performance of PETG-f over PETG-c is evident. The throughput of PETG-f is 42.2% higher than that of PETG-c on average (0.1%, 14.4%, 7.3%, 8.1%, 4.9%, -0.8%, 34.6%, 131.5%, 180.1%, respectively), while the average latency of PETG-f is 0.79× that of PETG-c on average (1.00×, 0.87×, 0.90×, 0.90×, 0.94×, 0.99×, 0.72×, 0.43×, 0.34×, respectively). PETG-f does not have deadlock in all cases. This indicates the advantage of the fine-granularity multi-level locking mechanism of PETGraphDB.

(2) The performance gap between PETG-f and PETG-c is widened as the number of concurrent requests exceeds 20. The transaction throughput decreases when the number of concurrent requests is larger than the number of physical cores of the machine, indicating the competition for computing resources. However, as the number of concurrent requests continuously increases after 20, the throughput of PETG-c exhibits a faster decline, while its latency and deadlock count exhibit a faster increase simultaneously. This indicates that the competition in transactions of PETG-c is for locks rather than computing resources, which is another evidence of the advantage of the fine-granularity multi-level locking mechanism of PETGraphDB.

VII. CONCLUSION

This paper presents PETGraphDB, a temporal graph data management system. PETGraphDB supports a native valid-time temporal property graph model, adapts to the data features and access patterns of the property evolution temporal graphs, and guarantees ACID properties. We extended the existing graph data management system (Neo4j) to support the data model and developed an efficient temporal property storage, transaction management, and a high-level query language. Experimental results using three temporal property graph datasets show that PETGraphDB can effectively and efficiently manage large-scale temporal graph data on a single machine with an average of 67% disk space-saving. The query latency of PETGraphDB surpasses the existing temporal graph data management solutions by 267 times on average. Besides, its transaction throughput is 58 times that of the current best solutions. This work provides valuable insights into the management of temporal graph data.

VIII. AI-GENERATED CONTENT ACKNOWLEDGEMENT

We improve the readability of the paper text using the functions provided by Grammarly (<https://grammarly.com>) in the text editor: (1)“Improve it”, (2)“Shorten it”, and (3) correct grammar errors and typos.

REFERENCES

- [1] M. E. J. Newman, “The structure and function of complex networks,” *SIAM Rev.*, vol. 45, no. 2, pp. 167–256, 2003. [Online]. Available: <https://doi.org/10.1137/S003614450342480>
- [2] L. d. F. Costa, O. N. Oliveira Jr., G. Travieso, F. A. Rodrigues, P. R. Villas Boas, L. Antunes, M. P. Viana, and L. E. Correa Rocha, “Analyzing and modeling real-world phenomena with complex networks: a survey of applications,” *Advances in Physics*, vol. 60, no. 3, pp. 329–412, Jun. 2011. [Online]. Available: <https://doi.org/10.1080/00018732.2011.572452>
- [3] P. Holme and J. Saramäki, “Temporal networks,” *Physics Reports*, vol. 519, no. 3, pp. 97–125, Oct. 2012. [Online]. Available: <http://linkinghub.elsevier.com/retrieve/pii/S0370157312000841>
- [4] H. Huang, J. Song, X. Lin, S. Ma, and J. Huai, “Tgraph: A temporal graph data management system,” in *Proceedings of the 25th ACM International Conference on Information and Knowledge Management, CIKM 2016, Indianapolis, IN, USA, October 24-28, 2016*. ACM, 2016, pp. 2469–2472. [Online]. Available: <https://doi.org/10.1145/2983323.2983335>
- [5] S. Ma, R. Hu, L. Wang, X. Lin, and J. Huai, “An efficient approach to finding dense temporal subgraphs,” *IEEE Trans. Knowl. Data Eng.*, vol. 32, no. 4, pp. 645–658, 2020. [Online]. Available: <https://doi.org/10.1109/TKDE.2019.2891604>
- [6] T. P. Peixoto and L. Gauvin, “Change points, memory and epidemic spreading in temporal networks,” *Scientific Reports*, vol. 8, no. 1, p. 15511, Oct. 2018. [Online]. Available: <https://www.nature.com/articles/s41598-018-33313-1>
- [7] S. Sarkar, R. Guo, and P. Shakarian, “Using network motifs to characterize temporal network evolution leading to diffusion inhibition,” *Social Network Analysis and Mining*, vol. 9, no. 1, p. 14, Apr. 2019. [Online]. Available: <https://doi.org/10.1007/s13278-019-0556-z>
- [8] X. Li, J. Han, J.-G. Lee, and H. Gonzalez, “Traffic Density-Based Discovery of Hot Routes in Road Networks,” in *Advances in Spatial and Temporal Databases*. Berlin, Heidelberg: Springer, 2007, pp. 441–459.
- [9] H. Chen, S. Ma, J. Liu, and L. Cui, “Discovery of temporal network motifs,” *IEEE Transactions on Knowledge and Data Engineering*, vol. 37, no. 5, pp. 2376–2390, 2025.
- [10] A. Li, S. P. Cornelius, Y.-Y. Liu, L. Wang, and A.-L. Barabási, “The fundamental advantages of temporal networks,” *Science*, vol. 358, no. 6366, pp. 1042–1046, 2017. [Online]. Available: <https://www.science.org/doi/abs/10.1126/science.aai7488>
- [11] T. V. Jensen and P. Pinson, “RE-Europe, a large-scale dataset for modeling a highly renewable European electricity system,” *Scientific Data*, vol. 4, no. 1, p. 170175, Nov. 2017. [Online]. Available: <https://www.nature.com/articles/sdata2017175>
- [12] M. Massri, Z. Miklos, P. Raipin, and P. Meye, “Clock-G: A temporal graph management system with space-efficient storage technique,” in *2022 IEEE 38th International Conference on Data Engineering (ICDE)*. Kuala Lumpur, Malaysia: IEEE, May 2022, pp. 2263–2276. [Online]. Available: <https://ieeexplore.ieee.org/document/9835183>
- [13] Y. Miao, W. Han, K. Li, M. Wu, F. Yang, L. Zhou, V. Prabhakaran, E. Chen, and W. Chen, “ImmortalGraph: A System for Storage and Analysis of Temporal Graphs,” *ACM Transactions on Storage*, vol. 11, no. 3, pp. 1–34, Jul. 2015. [Online]. Available: <http://dl.acm.org/citation.cfm?doid=2809503.2700302>
- [14] P. Jamkhedkar, T. Johnson, Y. Kanza, A. Shaikh, N. K. Shankaranarayanan, and V. Shkapenyuk, “A Graph Database for a Virtualized Network Infrastructure,” in *Proceedings of the 2018 International Conference on Management of Data*, ser. SIGMOD ’18. New York, NY, USA: ACM, 2018, pp. 1393–1405. [Online]. Available: <http://doi.acm.org/10.1145/3183713.3190653>
- [15] C. Cattuto, M. Quaggiotto, A. Panisson, and A. Averbuch, “Time-varying social networks in a graph database: a Neo4j use case,” in *First International Workshop on Graph Data Management Experiences and Systems*. New York New York: ACM, Jun. 2013, pp. 1–6. [Online]. Available: <https://dl.acm.org/doi/10.1145/2484425.2484442>
- [16] A. Debrouvier, E. Parodi, M. Perazzo, V. Soliani, and A. Vaisman, “A model and query language for temporal graph databases,” *The VLDB Journal*, vol. 30, no. 5, pp. 825–858, Sep. 2021. [Online]. Available: <https://link.springer.com/10.1007/s00778-021-00675-4>
- [17] A. Campos, J. Mozzino, and A. A. Vaisman, “Towards temporal graph databases,” in *Proceedings of the 10th Alberto Mendelzon International Workshop on Foundations of Data Management, Panama City, Panama, May 8-10, 2016*, ser. CEUR Workshop Proceedings, vol. 1644. CEUR-WS.org, 2016. [Online]. Available: <https://ceur-ws.org/Vol-1644/paper40.pdf>
- [18] G. Theodorakis, J. Clarkson, and J. Webber, “Aion: Efficient temporal graph data management,” in *Proceedings 27th International Conference on Extending Database Technology, EDBT 2024, Paestum, Italy, March 25 - March 28*. Paestum, Italy: OpenProceedings.org, 2024, pp. 501–514. [Online]. Available: <https://doi.org/10.48786/edbt.2024.43>
- [19] J. Hou, Z. Zhao, Z. Wang, W. Lu, G. Jin, D. Wen, and X. Du, “AeonG: An Efficient Built-in Temporal Support in Graph Databases,” *Proceedings of the VLDB Endowment*, vol. 17, no. 6, pp. 1515–1527, Feb. 2024. [Online]. Available: <https://dl.acm.org/doi/10.14778/3648160.3648187>
- [20] C. Rost, K. Gómez, M. Täschner, P. Fritzsche, L. Schons, L. Christ, T. Adameit, M. Junghanns, and E. Rahm, “Distributed temporal graph analytics with GRADOOP,” *The VLDB Journal*, vol. 31, no. 2, pp. 375–401, 2022. [Online]. Available: <https://doi.org/10.1007/s00778-021-00667-4>
- [21] J. Byun, S. Woo, and D. Kim, “ChronoGraph: Enabling Temporal Graph Traversals for Efficient Information Diffusion Analysis over Time,” *IEEE Transactions on Knowledge and Data Engineering*, vol. 32, no. 3, pp. 424–437, Mar. 2020. [Online]. Available: <https://ieeexplore.ieee.org/document/8606161/>
- [22] U. Khurana and A. Deshpande, “Storing and analyzing historical graph data at scale,” in *Proceedings of the 19th International Conference on Extending Database Technology, EDBT 2016, Bordeaux, France, March 15-16, 2016, Bordeaux, France, March 15-16, 2016*. OpenProceedings.org, 2016, pp. 65–76. [Online]. Available: <https://doi.org/10.5441/002/edbt.2016.09>
- [23] A. G. Labousseur, J. Birnbaum, P. W. Olsen, S. R. Spillane, J. Vijayan, J.-H. Hwang, and W.-S. Han, “The G* graph database: efficiently managing large distributed dynamic graphs,” *Distributed and Parallel Databases*, vol. 33, no. 4, pp. 479–514, Dec. 2015. [Online]. Available: <https://doi.org/10.1007/s10619-014-7140-3>
- [24] W. Han, Y. Miao, K. Li, M. Wu, F. Yang, L. Zhou, V. Prabhakaran, W. Chen, and E. Chen, “Chronos: a graph engine for temporal graph analysis,” in *Proceedings of the Ninth European Conference on Computer Systems - EuroSys '14*. Amsterdam, The Netherlands: ACM Press, 2014, pp. 1–14. [Online]. Available: <http://dl.acm.org/citation.cfm?doid=2592798.2592799>
- [25] R. Cheng, E. Chen, J. Hong, A. Kyrola, Y. Miao, X. Weng, M. Wu, F. Yang, L. Zhou, and F. Zhao, “Kineograph: taking the pulse of a fast-changing and connected world,” in *Proceedings of the 7th ACM european conference on Computer Systems - EuroSys '12*. Bern, Switzerland: ACM Press, 2012, p. 85. [Online]. Available: <http://dl.acm.org/citation.cfm?doid=2168836.2168846>
- [26] A. Bonifati, G. Fletcher, H. Voigt, and N. Yakovets, *Data Models*. Cham: Springer International Publishing, 2018, pp. 3–14. [Online]. Available: https://doi.org/10.1007/978-3-031-01864-0_2
- [27] H. Wu, J. Cheng, S. Huang, Y. Ke, Y. Lu, and Y. Xu, “Path problems in temporal graphs,” *Proceedings of the VLDB Endowment*, vol. 7, no. 9, pp. 721–732, May 2014. [Online]. Available: <http://dl.acm.org/citation.cfm?doid=2732939.2732945>
- [28] K. Kulkarni and J.-E. Michels, “Temporal features in SQL:2011,” *ACM SIGMOD Record*, vol. 41, no. 3, p. 34, Oct. 2012. [Online]. Available: <http://dl.acm.org/citation.cfm?doid=2380776.2380786>
- [29] Y. Wang, Y. Yuan, Y. Ma, and G. Wang, “Time-Dependent Graphs: Definitions, Applications, and Algorithms,” *Data Science and Engineering*, vol. 4, no. 4, pp. 352–366, Dec. 2019. [Online]. Available: <http://link.springer.com/10.1007/s41019-019-00105-0>
- [30] C. E. Dyreson, “Chronon,” in *Encyclopedia of Database Systems*, L. Liu

and M. T. Özsu, Eds. New York, NY: Springer, 2018, pp. 425–425. [Online]. Available: https://doi.org/10.1007/978-1-4614-8265-9_1050

[31] C. S. Jensen, C. E. Dyreson, M. Böhlen, J. Clifford, R. Elmasri, S. K. Gadia, F. Grandi, P. Hayes, S. Jajodia, W. Käfer, N. Kline, N. Lorentzos, Y. Mitsopoulos, A. Montanari, D. Nonen, E. Peressi, B. Pernici, J. F. Roddick, N. L. Sarda, M. R. Scalas, A. Segev, R. T. Snodgrass, M. D. Soo, A. Tansel, P. Tiberio, and G. Wiederhold, “The consensus glossary of temporal database concepts — February 1998 version,” in *Temporal Databases: Research and Practice*, G. Goos, J. Hartmanis, J. van Leeuwen, O. Etzion, S. Jajodia, and S. Sripada, Eds. Berlin, Heidelberg: Springer Berlin Heidelberg, 1998, vol. 1399, pp. 367–405. [Online]. Available: <http://link.springer.com/10.1007/BFb0053710>

[32] C. S. Jensen and R. T. Snodgrass, “Time series,” in *Encyclopedia of Database Systems*, L. Liu and M. T. Özsu, Eds. Boston, MA: Springer US, 2009, p. 3114. [Online]. Available: https://doi.org/10.1007/978-0-387-39940-9_3825

[33] ———, “Time sequence,” in *Encyclopedia of Database Systems*, L. Liu and M. T. Özsu, Eds. Springer US, 2009, p. 3113. [Online]. Available: https://doi.org/10.1007/978-0-387-39940-9_3822

[34] ———, “Temporal data models,” in *Encyclopedia of Database Systems*, L. Liu and M. T. Özsu, Eds. Boston, MA: Springer US, 2009, pp. 2952–2957. [Online]. Available: https://doi.org/10.1007/978-0-387-39940-9_394

[35] P. Terenziani and R. Snodgrass, “Reconciling point-based and interval-based semantics in temporal relational databases: a treatment of the telic/atelic distinction,” *IEEE Transactions on Knowledge and Data Engineering*, vol. 16, no. 5, pp. 540–551, 2004.

[36] Nadime Francis, A. Taylor, A. Green, P. Guagliardo, L. Libkin, T. Lindaaker, V. Marsault, S. Plantikow, M. Rydberg, and P. Selmer, “Cypher: An Evolving Query Language for Property Graphs,” in *Proceedings of the 2018 International Conference on Management of Data - SIGMOD '18*. Houston, TX, USA: ACM Press, 2018, pp. 1433–1445. [Online]. Available: <http://dl.acm.org/citation.cfm?doid=3183713.3190657>

[37] S. E. Dreyfus, “An Appraisal of Some Shortest-Path Algorithms,” *Operations Research*, vol. 17, no. 3, pp. 395–412, Jun. 1969. [Online]. Available: <http://pubsonline.informs.org/doi/abs/10.1287/opre.17.3.395>

[38] R. Elmasri, G. T. J. Wu, and Y.-J. Kim, “The time index—an access structure for temporal data,” in *Proceedings of the Sixteenth International Conference on Very Large Databases*. San Francisco, CA, USA: Morgan Kaufmann Publishers Inc., 1990, p. 1–12.

[39] A. Behrend, A. Dignös, J. Gamper, P. Schmiegelt, H. Voigt, M. Rottmann, and K. Kahl, “Period index: A learned 2d hash index for range and duration queries,” in *Proceedings of the 16th International Symposium on Spatial and Temporal Databases*, ser. SSTD ’19. New York, NY, USA: Association for Computing Machinery, 2019, p. 100–109. [Online]. Available: <https://doi.org/10.1145/3340964.3340965>

[40] D. Comer, “Ubiquitous b-tree,” *ACM Comput. Surv.*, vol. 11, no. 2, p. 121–137, Jun. 1979. [Online]. Available: <https://doi.org/10.1145/356770.356776>

[41] P. O’Neil, E. Cheng, D. Gawlick, and E. O’Neil, “The log-structured merge-tree (LSM-tree),” *Acta Informatica*, vol. 33, no. 4, pp. 351–385, Jun. 1996. [Online]. Available: <https://doi.org/10.1007/s002360050048>

[42] T. H. Cormen, C. E. Leiserson, R. L. Rivest, and C. Stein, *Introduction to Algorithms*, 3rd ed. Cambridge, MA, USA: MIT Press, 2009, ch. 2.3, pp. 29–42.

[43] “LevelDB,” Jan. 2025. [Online]. Available: <https://github.com/google/leveldb>

[44] “Snappy, a fast compressor/decompressor,” Jan. 2025. [Online]. Available: <https://google.github.io/snappy/>